Observation of shifts in total reflection of a light beam by a multilayered structure

O. Costa de Beauregard
Institut Henri Poincaré, 11 rue Pierre et Marie Curie, 75005 Paris, France

C. Imbert and Y. Levy
Institut d'Optique Théorique et Appliquée, Bâtiment 503, Université de Paris-Sud, 91405 Orsay, France
(Received 2 December 1975; revised manuscript received 7 July 1976)

A very strong amplification of both the longitudinal and the transverse shifts in total reflection of a light beam, rendering them easily observable, together with the filtering of the corresponding pair of polarization eigenmodes, has been obtained by using one single reflection at a multilayered interface. After presenting the general philosophy of this approach and summarizing the computational techniques used by one of us (Y. Levy), we describe the two experimental setups, and produce the photographic recording of our results. Some theoretical implications of these are very briefly discussed in our conclusion.

I. INTRODUCTION

It is now well known[1] that in total reflection of a light beam at a plane interface two shifts occur: a longitudinal shift[2] (Fig. 1) with two eigenvalues separating, as eigenfunctions, the transverse electric (TE) and the transverse magnetic (TM) modes, and a transverse shift (Fig. 2),[3] with two opposite eigenvalues separating, as eigenfunctions, the L and R modes that are circularly polarized (left and right) inside the evanescent wave.[4] More generally theoretical analyses[5] have shown that the image of a rectilinear object normal to the beam and oblique on the incidence plane should consist of two parallel lines with orthogonal elliptical polarizations.[6]

Since they are small, the longitudinal[2] and the transverse[3] shifts have previously been rendered observable in two different sorts of setups using many successive total reflections. Both classes of multiplying procedures are in fact mutually incompatible, as should be expected, owing to the incompatibility of expansions of the polarization state of the beam in terms of linear or of circular polarizations.

In this paper we present, together with the experimental results, a new technique for displaying the longitudinal[7] and the transverse[8] shifts in a total reflection at one single interface, comprising the filtering of the two eigenmodes of the polarization state. The calculation of the apparatus by two of us (Y. Levy and C. Imbert) has used, for the longitudinal shift,[9,10] both the energy-flux[11] and the stationary-phase[12] method. For the transverse shift the calculation by the energy-flux method[3] is straightforward[13] and consistent with our measurements; it is not immediately evident, however, how the stationary-phase argument[14] can explain the amplification of the shift by means of the multiple layers.[15]

As a criterion for calculating our multilayered amplifying apparatus, the simple Renard[11] and Imbert[3] energy-flux-conservation formulas have been used. Denoting $z=0$ the "first interface" separating [Figs. 3(a) and 3(b)] the medium Ω_1, $z<0$, of index n_1 containing the plane incident and reflected waves from the following layers, $y=0$ incidence plane, $\vec{S}$ the Poynting vector, we write the longitudinal Δx and transverse Δy shifts as

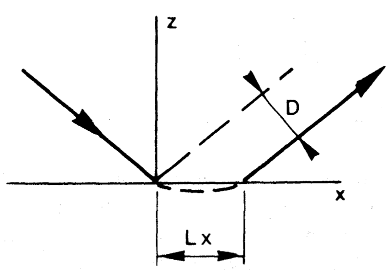

FIG. 1. The longitudinal or Goos-Hänchen shift.

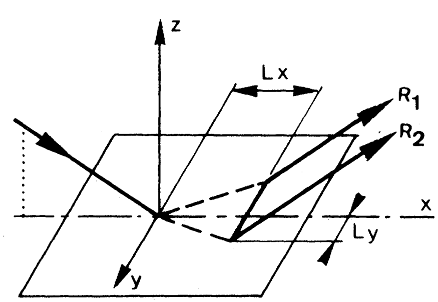

FIG. 2. Schematic representation of the longitudinal and the transverse shifts (in fact they are not simultaneously observable, as their eigenmodes belong to two different orthogonal sets).

$$\Delta x = \frac{1}{S_{1z}} \int_0^{+\infty} S_x dz \, , \tag{1}$$

$$\Delta y = \frac{1}{S_{1z}} \int_0^{+\infty} S_y dz \, , \tag{2}$$

that is, we take into account the longitudinal and transverse energy fluxes in all the layers Ω_p of indexes n_p, $p > 1$, including of course the final medium containing the evanescent wave; $\vec{S}_1$ denotes the Poynting vector inside the first medium [Figs. 3(a) and 3(b)].

We are thus led to discuss the expressions of $S_x(z)$ and $S_y(z)$. To this end, that solution of Maxwell's equations which, by hypothesis, is "evanescent" in z for $z > z_{P+1}$ and is harmonic in both the t and the x variables, must be displayed; Ω_{P+1} denotes the last medium [Figs. 3(a) and 3(b)].

II. LONGITUDINAL AND TRANSVERSE ENERGY FLUXES IN THE EVANESCENT SOLUTION OF MAXWELL'S EQUATIONS

The general solution[16] of the type we are considering can be displayed as an arbitrary superposition of a TE and a TM mode of expression (in units such that $c = 1$)

$$E_y = e^{i(\omega t - kx + e)} E(z) \, , \tag{3a}$$

$$H_y = e^{i(\omega t - kx + h)} H(z) \, . \tag{3b}$$

The temporal frequency ω and the spatial frequency k along x are common to both modes, and by hypothesis

$$k > \omega \quad \text{or} \quad k/\omega > 1 ; \tag{4}$$

e and h denote two phase constants, and $E(z)$ and $H(z)$ two functions that are continuous, except at the interfaces $z = z_p \, (p = 1, 2, \ldots, P)$.

According to whether the index of the pth layer Ω_p comprised between z_{p-1} and z_p is larger or smaller than $k/\omega > 1$, E and H are of the "homogeneous" type "sine and cosine," or of the "inhomogeneous" type "sinh and cosh," that is,

$$(E, H) = A_{e,h} \times \begin{Bmatrix} \sin(|l_p| z) \\ \sinh(|l_p| z) \end{Bmatrix} + B_{e,h} \times \begin{Bmatrix} \cos(|l_p| z) \\ \cosh(|l_p| z) \end{Bmatrix} \begin{matrix} \text{if } n_p > k/\omega > 1 \\ \text{if } 1 < n_p < k/\omega \end{matrix} \tag{5}$$

with by definition

$$l_p^2 = n_p^2 \omega^2 - k^2 \, . \tag{6}$$

By hypothesis $n_1 > k/\omega$, $n_{P+1} < k/\omega$, and in the last medium $z > z_{P+1}$, the wave has the expression

$$E(z) = E_0 e^{-lz}, \quad H(z) = H_0 e^{-lz} , \tag{7}$$

with E_0 and H_0 real; in fact,

$$n_{P+1} = 1 \, , \quad l^2 = \omega^2 - k^2 \, . \tag{8}$$

From (3a), (3b), and Maxwell's equations we obtain, ϵ_p and μ_p denoting the electric and magnetic constants,

$$\mu_p \omega H_x = -i\partial_z E y \, , \quad \mu_p \omega H_z = k E_y \, , \tag{9a}$$

$$\epsilon_p \omega E_x = i\partial_z H_y \, , \quad \epsilon_p \omega E_z = -k H_y \, . \tag{9b}$$

Denoting $n_p^2 = \epsilon_p \mu_p$ and

$$\sqrt{2} L = E_y + i H_y \, , \quad \sqrt{2} R = E_y - i H_y \, , \tag{10}$$

the expressions of the longitudinal and the transverse components of the Poynting vector

$$\vec{S} = \tfrac{1}{4} (\vec{E}^* \times \vec{H} + \vec{E} \times \vec{H}^*) \tag{11}$$

are thus

$$S_x = \frac{\omega}{2k} n_p^2 (E_y^* E_y + H_y^* H_y) \, , \tag{12}$$

$$S_y = \frac{k}{2 n_p^2 \omega^2} \frac{d}{dz} (L^* L - R^* R) \, . \tag{13}$$

As in the case of total reflection at a single interface,[4] formulas (12) and (13) express S_x and S_y as a canonical mean value with orthogonal eigenstates displayed. Thus we have the conclusion that the observation of the longitudinal shift of expression (1) should filter the two principal linear polarization modes, and that the observation of the trans-

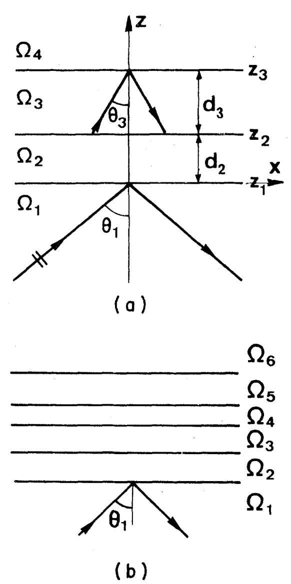

FIG. 3. Multilayered reflecting device for amplifying (a) the longitudinal and (b) the transverse energy flux; the wave propagating inside a layer is either of the homogeneous (sine and cosine), or of the inhomogeneous (sinh and cosh) type.

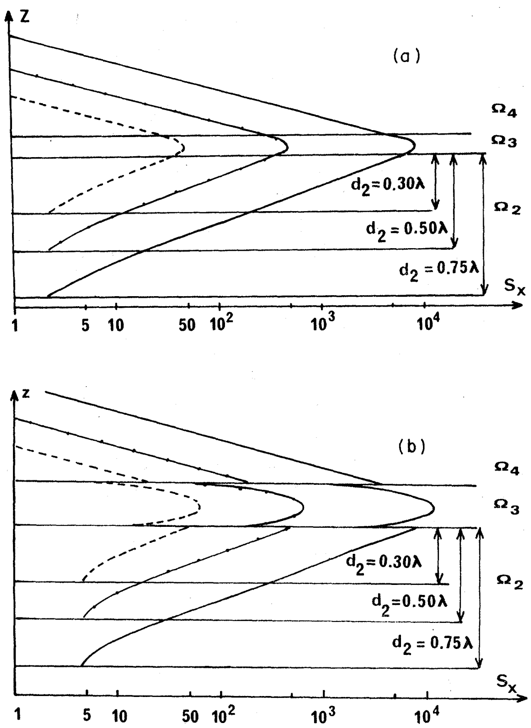

FIG. 4. 4-layered reflecting prism: This figure shows the z dependence of the longitudinal component S_x of the Poynting vector for (a) the transverse electric and (b) the transverse magnetic mode. The three curves correspond to different thicknesses of the layer Ω_2 (λ, wavelength *in vacuo*, incident wave with amplitude unity).

verse shift of expression (2) should filter the two orthogonal modes which are circularly polarized inside the last evanescent wave (inside the layer Ω_{P+1} such that $z > z_{P+1}$). As we shall see in Secs. V and VI these conclusions have been experimentally verified.

III. AMPLIFICATION OF THE LONGITUDINAL SHIFT

The stratified medium we have calculated and used is shown in Fig. 3. The incidence angle in Ω_1 and the indexes in Ω_1, Ω_2, and Ω_3 are such that the wave is of the homogeneous type in Ω_1 and Ω_3 and of the inhomogeneous type in Ω_2 and Ω_4. It has been shown that the amplitudes of the propagating waves in Ω_3 are very large when the condition[10a]

$$4\pi(d_3/\lambda)n_3\cos\theta_3 - \psi_{31} - \psi_{34} = 2m\pi \tag{14}$$

is satisfied; d_3/λ is the ratio of the thickness of the layer Ω_3 to the wavelength of the radiation in the vacuum, θ_3 is the angle of refraction in Ω_3, ψ_{31} and ψ_{34} are the phase shifts between the incident and reflected waves in Ω_3, at total reflection, respectively, upon the two faces of Ω_3, and m denotes the integer. For weak coupling ($l_2d_2 > 1$)

$$\psi_{31} = \psi_{32} + 2\sin\psi_{32}\cos\psi_{12}\exp(-2l_2d_2)\,.$$

This relation shows the thickness dependence of Ω_2 on the phase shift ψ_{31}. When l_2d_2 becomes infinite, ψ_{31} goes to ψ_{32}, which is the phase shift on the interface between Ω_3 and Ω_2, with Ω_2 a semi-infinite medium.[10b] If condition (14) is satisfied, the amplitude of the evanescent wave in the last medium Ω_4 is very large. In the general case, the expression of ψ_{31} should be derived from the reflection coefficient of a system consisting of two semi-infinite media Ω_3, Ω_1 separated by the layer Ω_2. The light is incident from Ω_3 to Ω_1 at the incidence angle θ_3. Since the phase shifts are different for the TE and the TM modes, the resonance condition (14) can be obtained only for one of these two modes. Figure 4(a) displays for three different values of the thickness d_2 of Ω_2 the longitudinal S_x component of the Poynting vector in the TE mode as a function of z (where the amplitude of the incident wave is taken as unity). It is seen that S_x attains very high values inside Ω_3, and at the interfaces of Ω_3, yielding an extremely strong longitudinal flux; let us recall that with only one interface S_x would hardly reach the value 12, as compared with the 10^3 to 10^4 obtained here. Figure 4(b) is the analogous one for the TM mode.

Table I displays, for five different values of d_2, the value Δx of the longitudinal, or Goos-Hänchen, shift, calculated by means of formulas (1) and (12), for the TE and the TM modes. As previously

TABLE I. Amplification of the longitudinal shift: values of the shift as depending on significant parameters of the 4-media reflecting prism. $\theta_1=70$ degrees, $n_1=1.72$, $n_2=1.330\,00$, $n_3=2.3000$, $n_4=1$, $\lambda=6328$ Å, λ is the wavelength of light *in vacuo*.

	TE Mode			TM Mode		
d_3/λ	$\Delta x/\lambda$	$\Delta' x/\lambda$	d_2/λ	$\Delta x/\lambda$	$\Delta' x/\lambda$	d_3/λ
0.111 90	6.6	6.6	0.25	9.9	10.0	0.226 48
0.112 81	11.7	11.7	0.30	17.6	17.9	0.228 05
0.113 58	36.8	37.8	0.40	55.2	56.3	0.229 42
0.113 73	65.4	66.2	0.45	98.3	99.4	0.229 70
0.113 82	117.6	118.5	0.50	174.6	177.3	0.229 85

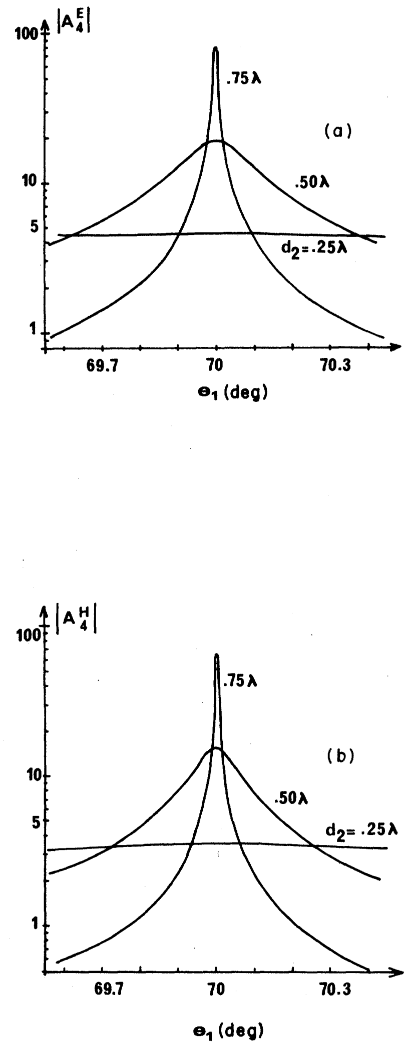

FIG. 5. 4-layered reflecting prism: This figure shows the incidence-angle dependence of the amplitude of the evanescent wave for (a) the transverse electric and (b) the transverse magnetic modes. The three curves correspond to different thicknesses of the layer Ω_2.

explained, the appropriate values of d_3/λ are different in both cases, and have been indicated.

For comparison, Table I includes also the values $\Delta' x$ of the longitudinal shift as calculated by means of the stationary-phase method, that is, by Artmann's formula[12]

$$\Delta' x/\lambda_1 = -\frac{1}{2\pi}\frac{d\psi}{d\theta_1}, \tag{15}$$

where θ_1 denotes the incidence angle in the medium Ω_1. It is seen that the agreement between the values given by Renard's formula (1) and by Artmann's formula (15) is extremely good. The values of the indices are also indicated in the table.

Formulas (1) and (12) show that the value of the longitudinal shift Δx depends on the absolute value of the field's amplitudes in the last medium, the variations of which with respect to the incidence angle around 70° is displayed in Fig. 5(a) for the transverse electric and Fig. 5(b) for the transverse magnetic modes. The three curves correspond to three different thicknesses of the first layer. The corresponding thicknesses of the second layer are calculated through formula (14), with the computed values given in Table I.

Formula (15) gives the value of Δx in terms of the slope $d\psi_1/d\theta_1$. Figures 6(a) and 6(b) display the variations of this slope for the three arrangements previously described.

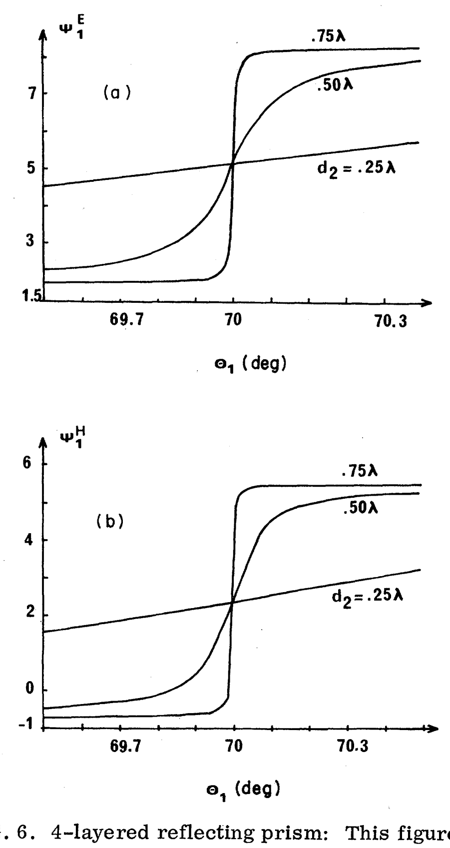

FIG. 6. 4-layered reflecting prism: This figure shows the incidence-angle dependence of the phase shifts between the incident and the reflected waves for (a) the transverse electric and (b) the transverse magnetic modes. The three curves correspond to three different thicknesses of the layer Ω_2. The phases are referred to one of the evanescent waves. Notice that the curves are slightly nonsymmetrical.

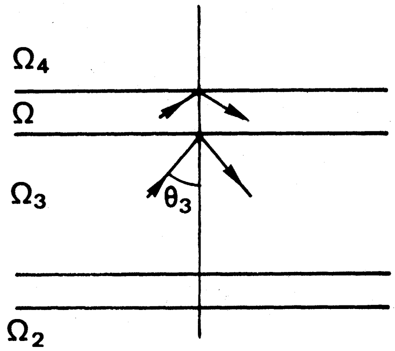

FIG. 7. In order to bring into coincidence the resonance angles for the transverse electric and the transverse magnetic modes, we replace the layer Ω_3 of the 4-layered prism by an ensemble of three appropriate layers, thus obtaining a 6-layered prism.

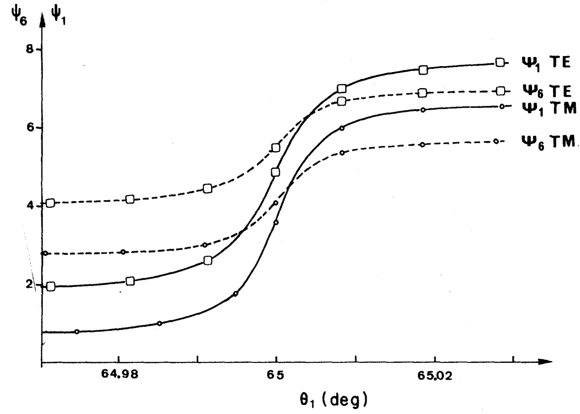

FIG. 9. 6-layered reflecting prism: This figure shows the incidence-angle dependence of the phase shifts ψ_1 of the reflected wave and ψ_6 of the (final) evanescent wave.

IV. AMPLIFICATION OF THE TRANSVERSE SHIFT

Two significant remarks can be made concerning formula (13). The first one is that, for amplifying the transverse shift, the resonance condition must be obtained (or at least approached) for *both* the TE and the TM modes, and this will imply the use of more than two intermediate layers.

The second remark is that the computation of the transverse shift using formula (13) is much simpler than that of the longitudinal shift using formula (12). Owing to the presence in (13) of the derivative d/dz it is sufficient for computing S_y (thus Δy) to take into account the values of the fields at both faces of each interface (through which they are discontinuous).

Consider for instance the case of the pure L mode, which by definition is such that $R=0$ or $E_y = iH_y$. Then $L^*L - R^*R = L^*L = 4E_y^*E_y = 4H_y^*H_y$. A similar remark had been made previously by one of us.[3]

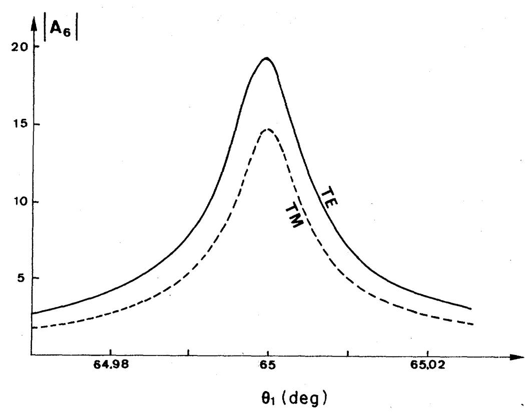

FIG. 8. 6-layered reflecting prism: This figure shows the incidence-angle dependence of the amplitude of the evanescent wave for (a) the transverse electric and (b) the transverse magnetic modes, $d_2 = 0.6\lambda$, incidence wave with amplitude unity.

One of us (Y. Levy) has found that by replacing the layer Ω_3 of Fig. 3(a) by an appropriate set of three layers (Fig. 7), the resonance condition can in principle be simultaneously met for both the TE and the TM modes. If realized, such a setup would in fact be the first device amplifying both the longitudinal and the transverse shifts. In connection with previous remarks concerning the complementarity between the longitudinal and the transverse shifts, one need not say that a theoretical and experimental study of the image of a point source, together with the polarization states of its different points, would then be extremely interesting.

Owing to the obvious difficulty in producing the appropriate 6-media (5 interfaces) amplifying device (Figs. 8, 9, 10), we have been able to obtain up to now only an approximate realization of the theoretical definition, yielding in fact a very strong amplification of the TE *or* the TM mode for two slightly different incidence angles. This obviously does not "bring into focus" the complementarity problem of the TE and the TM modes; nevertheless, it has allowed us[8,13] to obtain a very strong amplification of the transverse shift, together with an easily observable separation of the two corresponding eigenmodes, L and R, which we discuss in Sec. VI.

Presently we summarize the technique for defining[13] a 6-media amplifying device producing simultaneous resonance of the TE and the TM modes.

We go back to formula (14) with the idea that, without changing the values of ω and k in formulas (3a) and (3b) (i.e., the damping factor l of the final

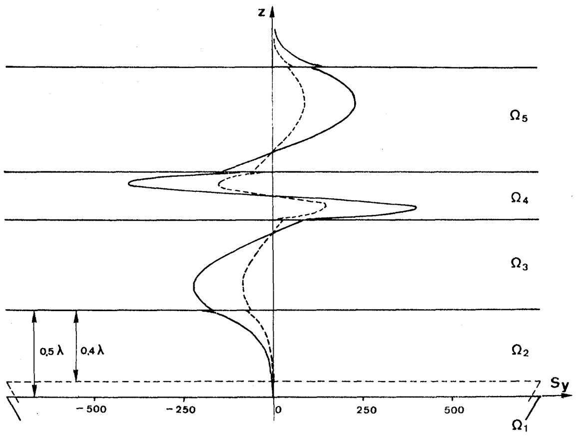

FIG. 10. 6-layered reflecting prism: z dependence of the transverse component S_y of the Poynting vector for two different thicknesses of the layer Ω_2. These are calculated curves corresponding to the ideal case where resonance occurs at the same angle for the TE and the TM modes.

evanescent wave), we can produce a phase shift by replacing the interface between Ω_4 and Ω_3 by an appropriate new layer Ω (Fig.7), where the wave will be of the homogeneous type. With θ denoting the propagation angle in this layer, one easily finds that the phase shifts ψ_{34}^E of the TE mode and ψ_{34}^H of the TM mode will be rendered equal if

$$n^2 = n_3 n_4 \quad and \quad 4nd\cos\theta = \lambda . \tag{25}$$

Similarly, by replacing the interface between Ω_3 and Ω_2 by an appropriate layer, it is possible to render equal the phase shifts ψ_{31}^H and ψ_{31}^E. In this case, however, the presence of the first medium Ω_1 must be taken into account. But as it is thick when the amplification is strong, its influence on the phase shifts is then small.

The final definition of the 6-media amplifying device is contained in the first four columns of Table II. The last column gives the calculated absolute value of the transverse shift, for pure circular polarization inside the last evanescent wave, as a function of the thickness of the layer Ω_2.

In Table II the values of the refraction indices and the thicknesses of the layers are slightly different from those calculated through formula (25). This is because we had to use the available transparent media, deposited *in vacuo*, approaching at best those defined theoretically.

Things being so, the thicknesses of the two layers have been readjusted so that the phase shifts ψ_{31}^E and ψ_{31}^H, together with ψ_{34}^E and ψ_{34}^H, are, respectively, equal to each other. The values given in Table II have been computed according to this situation.

TABLE II. Amplification of the transverse shift: values of the shift as depending on significant parameters of the 6-media reflecting prism. $n_1 = 1.700\,00$, $n_2 = 1.330\,00$, $n_3 = 1.600\,00$, $n_4 = 2.330\,00$, $n_5 = 1.600\,00$, $n_6 = 1$, λ is the wavelength *in vacuo*.

d_2/λ	d_3/λ	d_4/λ	d_5/λ	$\Delta y/\lambda$
0.500 00	0.491 68	0.270 09	0.601 16	15.5
0.600 00	0.491 97	0.270 02	0.601 97	42.4
0.700 00	0.492 25	0.269 99	0.602 09	116.5
0.800 00	0.492 10	0.269 99	0.602 33	325.4

Table II displays the values of the transverse shift Δy, as computed from values of the refracting indices intended to be the experimental ones. It is seen that Δy depends strongly on the thickness of the first layer, so that any error in the realization of this thickness affects badly the result.

The result also critically depends on the thicknesses of the other layers, because, as previously explained, for amplifying the transverse shift it is necessary to amplify *both* the TE and the TM modes [as is obvious in formulas (10) and (13)]. Any error on the thicknesses of the layers Ω_3, Ω_4, and Ω_5 will entail a separation of the resonance angles for the TE and the TM modes, and will thus severely reduce the amplification ratio. This we have verified by numerical computations.

V. EXPERIMENTAL OBSERVATION OF THE LONGITUDINAL SHIFT

The amplifying prism, as defined in Sec. II (for use in the TE mode) is shown in Fig. 11. Figure 12 shows how the existence of two images of a rectilinear object AB orthogonal to the incidence planes is predicted: The shifted image $A''B''$ is produced by those rays which, incident at the resonant value Θ_1 of the incidence angle θ_1, go through the amplifying device; the nonshifted image $A'B'$ is produced both by the rays of the incidence angle Θ_1 that are directly reflected by the first interface QR, and by the rays of incidence angles $\theta_1 \neq \Theta_1$ which do not undergo the strong tunnel effect.

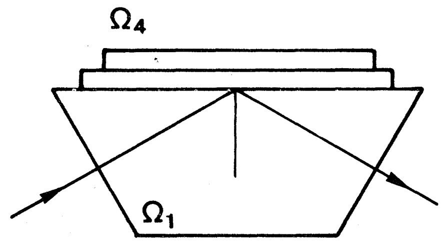

FIG. 11. The 4-layered reflecting prism for producing the longitudinal shift.

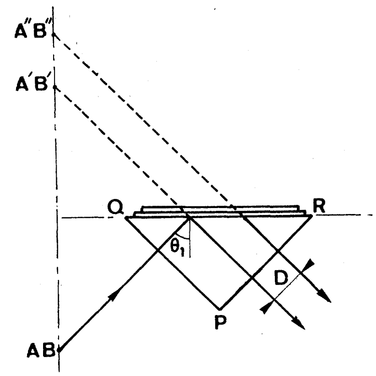

FIG. 12. Tunneling and nontunneling photons and the longitudinally shifted, and the nonshifted, reflected rays.

Figure 13 displays the overall experimental setup, comprising a linear polarizing laser, an orientable half-wave plate L_1, a converging lens O_1, a half-wave plate L_2 covering half of the beam with its axis at 45°, the linear object, the prism, and a lense O_2 producing the final image. With the appropriate orientation of L_1 we obtain, after L_2, a TE polarization on one semiplane ((I), and a TM polarization on the other one (II). By a 45° rotation of L_1 we can exchange these polarizations.

The thickness of the first layer was $d_2 = 0.45\lambda$, the computed value of the longitudinal shift Δx then being 42 μ. The experimental value of d_2 has been $0.45\lambda \pm 5\%$.

With a laser yielding the wavelength $\lambda = 6328$ Å, and a resonance incidence angle of approximately 71°, the measured shift has been 45 μ (which is comparable to the value produced by some 50 total reflections at a single interface).

Table I shows that the theoretical value of Δx depends strongly on d_2; for $d_2 = 0.5\lambda$ one finds $\Delta x \simeq 75$ μ.

In our experiment the object was a Wolter plate,[17] as in a previous work by one of us,[3] producing a π phase difference between two semiplanes and easily yielding a fine dark straight line as object.

Figures 14(a), 14(b), and 14(c) display the photographic recording of the image of this object, and show both a nonshifted and a shifted image, as explained above. Of course, no Δx shift appears with the TM mode. The experimental value of Δx is the distance between the nonshifted and the shifted image. As expected, the observed Δx (Refs. 7, 12) strongly depends on the incidence angle, and appears only for the resonance value.

By rotating the half-wave plate we have also verified that the shift exists only for the principal linear polarization mode to which the amplifying device is adapted (that is, the TE mode in the case we are considering).

Figures 14(a), 14(b), and 14(c) display the photographic recording, with three different orientations of L_1: Fig. 14(a) above, TE mode, below, TM mode; Fig. 14(b) above, TM mode, below, TE mode; Fig. 14(c) plate L_2 removed and incident linear polarization at 45° of the incidence plane.

VI. EXPERIMENTAL OBSERVATION OF THE TRANSVERSE SHIFT

The device (Fig. 15) we have obtained is not identical to its theoretical specification, the theoretical values of the thicknesses of which are given in the third line of Table II, ±5%. Instead of the theoretical angular separation 0 between the two resonance angles of ≃63°, we have obtained 0.2°. And, instead of the calculated value ≃80 μ for Δy, we have measured $\Delta y \simeq 30$ μ. This is nevertheless 100 times larger than the value predicted in total reflection at a single interface.

In such conditions the two eigenmodes of the transverse shift, that is, those which are circularly polarized inside the final evanescent wave, are, in both the incident and the reflected beams, elliptical modes which are symmetrical to each other with respect to the incidence plane and have extremely unequal axes; at the resonance angle Θ_{1E} they are extremely close to the TE or $\perp$ mode, and at the resonance angle Θ_{1H} they are extremely close to the TM or $\|$ mode [Figs. 16(a) and 16(b)]. It thus follows that *practically* a beam with linear polarization $\|$, incident at the resonance angle Θ_{1E}, and that a beam with linear polarization $\perp$, incident at the resonance angle Θ_{1H}, will excite both eigenstates of the transverse shift, whereas the opposite associations will not be able to display the transverse shift.

Figure 17 explains (in analogy with the analysis appropriate for the longitudinal shift) why 3 images of a linear object AB placed inside the incidence plane are predicted. The rays incident at the resonance angle Θ_{1E} or Θ_{1H} will (provided the other mode $\perp$ or $\|$ is, respectively, present also) yield

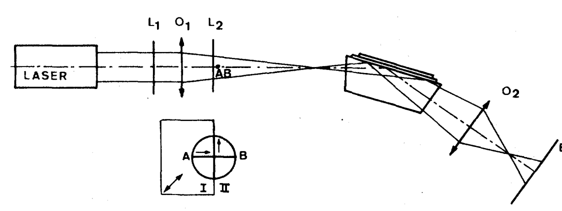

FIG. 13. Overall experimental setup for producing and observing the longitudinal shift, where L_1 is an orientable half-wave plate, L_2 is a half-wave plate covering half of the beam with axis at 45°, and AB is a linear object orthogonal to the incidence plane.

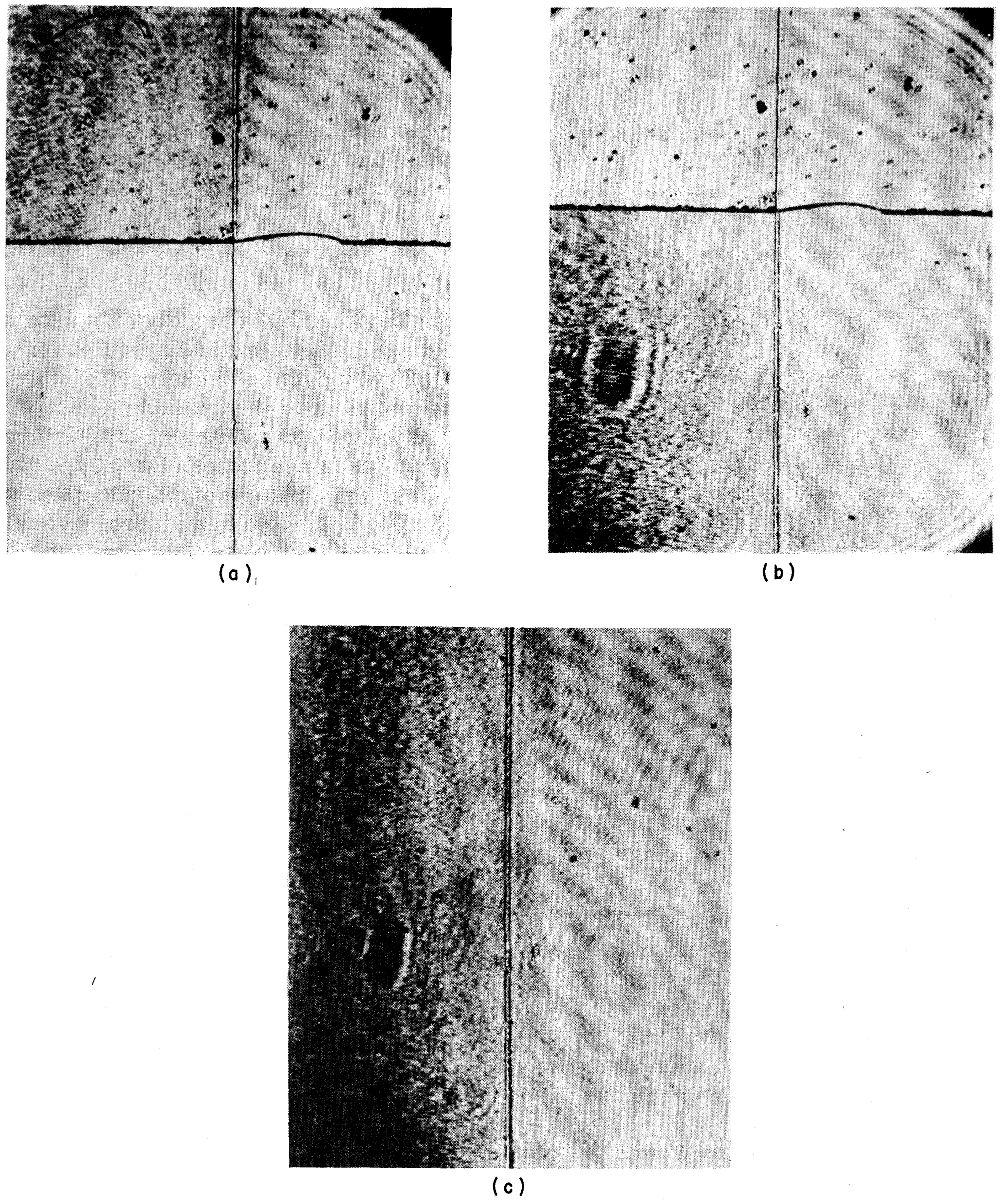

FIG. 14. Photographic recording of the longitudinal shift, where (a) above shows the TE mode and below the TM mode, (b) above shows the TM mode and below the TE mode, and (c) shows the linear polarization at 45°.

two symmetrically shifted images $A_1''B_1''$ and $A_2''B_2''$. The rays which do not have the good incidence angle will not undergo the large tunnel effect and will produce a nonshifted image $A'B'$.

Figure 18 shows the overall experimental apparatus, comprising a nonpolarized laser, an orientable linear polarizer, a converging lens, a linear object placed inside the incidence plane, the multiplying prism, and a lens producing the final image.

We[8,13] have used in succession two linear objects. First a Wolter plate, as in our study of the longi-

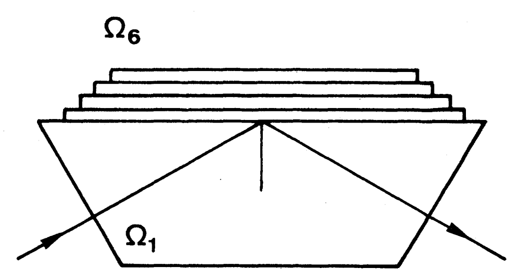

FIG. 15. The 6-layered reflecting prism for producing the transverse shift.

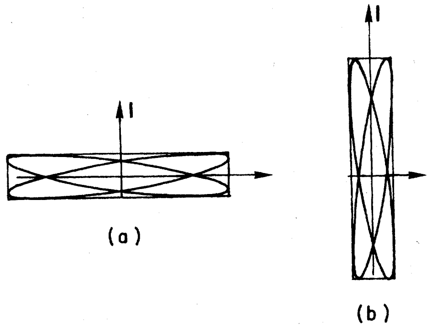

FIG. 16. The eigenmodes of the transverse shift (circularly polarized inside the last evanescent wave) as observed in the incident or the reflected plane wave (very elongated elliptical polarizations) for (a) the resonance angle for quasi-TE excitation and (b) the resonance angle for quasi-TM excitation.

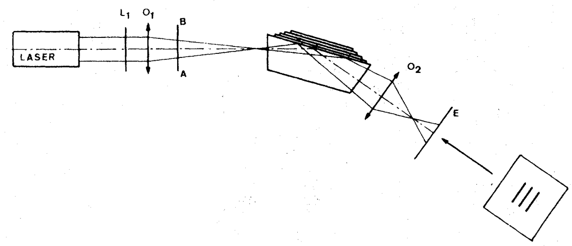

FIG. 18. Overall experimental setup for producing and observing the transverse shift, where L_1 is an orientable linear polarizer and AB is a linear object inside the incidence plane.

tudinal shift. Figure 19 is the corresponding photographic recording of the final image. As was expected it shows three lines, the central, nonshifted, one, being the trace of the incidence plane and the natural reference for measuring the transverse shift. The two symmetrically shifted lines are at a measured distance of 30 μ from the central line. We have verified that the transverse shift depends critically on the incidence angle, and appears only inside an extremely narrow range around the resonance value.

By rotating the linear-polarization analyzer we have verified that (as explained previously) the polarization of the two shifted lines is indiscernible from the linear polarization either parallel or perpendicular to the incidence plane (depending on which value of the resonance angle we are using), whereas the polarization of the nonshifted line is similar to that of the incident beam.

We have also used as object a slit of width 30 μ. The photographic recording of its image is shown in Fig. 20. It also consists of three strips, the central one being in fact slightly brighter than the two lateral ones. The other comments are similar to those pertaining to the previous case.

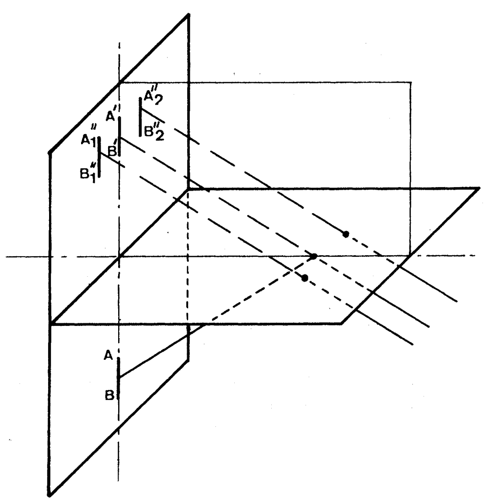

FIG. 17. Tunneling and nontunneling photons for the two transversally shifted $A''_1B''_1$, $A''_2B''_2$ and the nonshifted $A'B'$ images; AB is a linear object inside the incidence plane.

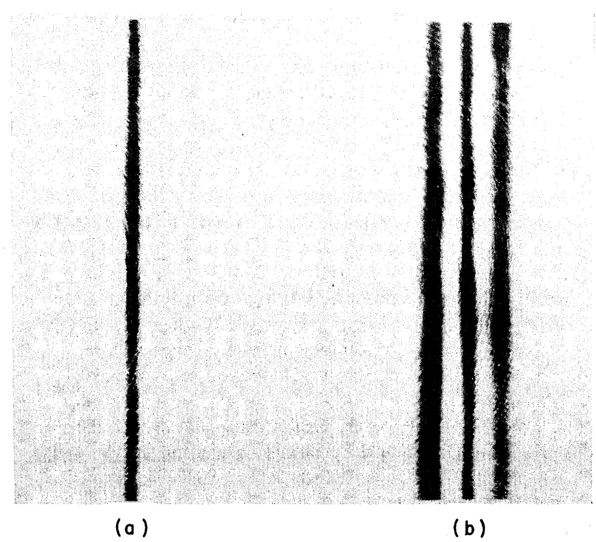

FIG. 19. Photographic recording of the transverse shift with a Wolter plate as object for (a) nonresonant and (b) resonant reflection, showing a nonshifted and two shifted images. The measured value of the transverse shift, that is, the distance between the two lateral lines and the central one, is 30 $\mu \pm 2\%$.

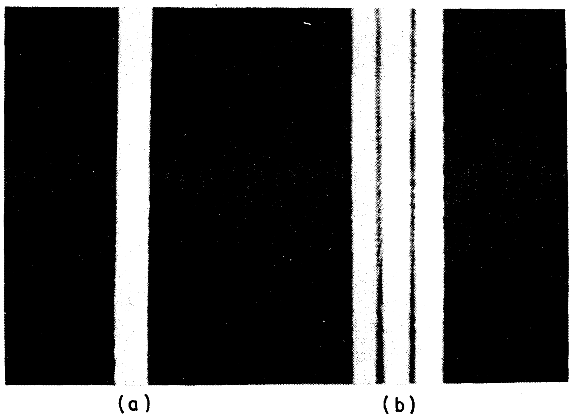

FIG. 20. Photographic recording of the transverse shift (same as Fig. 19), but with a narrow slit replacing the Wolter plate. This photograph has not been used for measuring the transverse shift.

VII. CONCLUSIONS

A new approach, both theoretical and experimental, has been presented here for studying the longitudinal and transverse shifts in total reflection of a light beam. It has been proved,[7,8,13] both theoretically and experimentally, that both shifts can be rendered clearly visible by one single reflection in a multilayered reflecting prism.

While this result needs little commentary in the longitudinal case and confirms analogous independent research,[9] it has, in the transverse case, implications that should perhaps be emphasized.

The experimental results presented in Sec. VI of the present work, together with the theoretical definition of the multiplying prism given in Sec. IV and the analysis in Sec. II, definitely show the existence of a quantized transverse shift produced by the transverse energy flux inside an elliptically polarized evanescent wave (its eigenfunctions are the circular polarizations). Moreover, it is not at all clear at first sight[15] how the stationary-phase method[18] can explain the very large values of the transverse shift as displayed by our multilayered reflecting prism.

This definitely proves, in our opinion, that the energy flow in our experiment is oblique on the phase planes, that is, noncollinear to the real part of the complex momentum $\hbar\vec{k}$ of the "evanescent photons." This "quantal momentum" $\hbar\vec{k}$ is the analog, in the present case, of the "Minkowski momentum"[19] of the photon inside a refracting medium, while the "Abraham-type momentum"[20] is collinear to the Poynting vector and the energy flux.[21]

[1] H. K. Lotsch, Optik (Stuttgart) 32, 116 (1970); 32, 189 (1970); 32, 299 (1971); 32, 553 (1971) give many references.

[2] F. Goos and H. Hänchen, Ann. Phys. (Leipzig) 1, 333 (1947); 5, 251 (1949); A. Mazet, C. Imbert, and S. Huard, C. R. Acad. Sci. Ser. B 273, 592 (1971).

[3] C. Imbert, Phys. Rev. D 5, 787 (1972).

[4] O. Costa de Beauregard and C. Imbert, Phys. Rev. Lett. 28, 1211 (1972); Phys. Rev. D 7, 3555 (1973).

[5] M. Steers and J. Billard, C. R. Acad. Sci. Ser. B 276, 455 (1973); J. Ricard, Nouv. Rev. Opt. 7, 1 (1976).

[6] J. M. Jauch and F. Rohrlich, *The Theory of Photons and Electrons* (Addison-Wesley, Cambridge, Mass., 1955), pp. 40–45, give a very clear analysis of this concept, which goes back to Fresnel and Arago.

[7] Y. Levy and C. Imbert, C. R. Acad. Sci. Ser. B 275, 723 (1972).

[8] Y. Levy and C. Imbert, Opt. Commun. 13, 43 (1975).

[9] J. E. Mindwinter and F. Zernecke, Appl. Phys. Lett. 16, 198 (1970); J. E. Mindwinter, IEEE J. Quant. Elect. 6, 583 (1970).

[10] (a) P. K. Tien, R. Ulrich, and R. Martin, Appl. Phys. Lett. 14, 291 (1969); (b) Y. Levy, Nouv. Rev. Opt. 3, 25 (1972).

[11] R. H. Renard, J. Opt. Soc. Am. 54, 1190 (1964).

[12] K. Artmann, Ann. Phys. (Leipzig) 12, 87 (1948).

[13] Y. Levy, Ph.D. thesis, Université de Paris VI (unpublished).

[14] H. Schilling, Ann. Phys. (Leipzig) 16, 122 (1965).

[15] J. Ricard and C. Vassalo (private communication).

[16] O. Costa de Beauregard, Opt. Commun. 13, 350 (1975).

[17] H. Wolter, Handb. Phys. 24, 582 (1956).

[18] D. G. Boulware, Phys. Rev. D 7, 2375 (1973); N. Ashby and S. C. Miller, *ibid.* 7, 2383 (1973); B. Julia and A. Neveu, J. Phys. (Paris) 34, 335 (1973).

[19] H. Minkowski, Nachr. Ges. Wiss. Göttingen, Math. Phys. Kl. Fachgruppe 2: 53 (1908); Ann. Math. 68, 472 (1910).

[20] M. Abraham, Rendic. Circ. Mat. Palermo 28, 1 (1909); 30, 33 (1910).

[21] O. Costa de Beauregard, C. Imbert, and J. Ricard, Int. J. Theor. Phys. 4, 125 (1971).

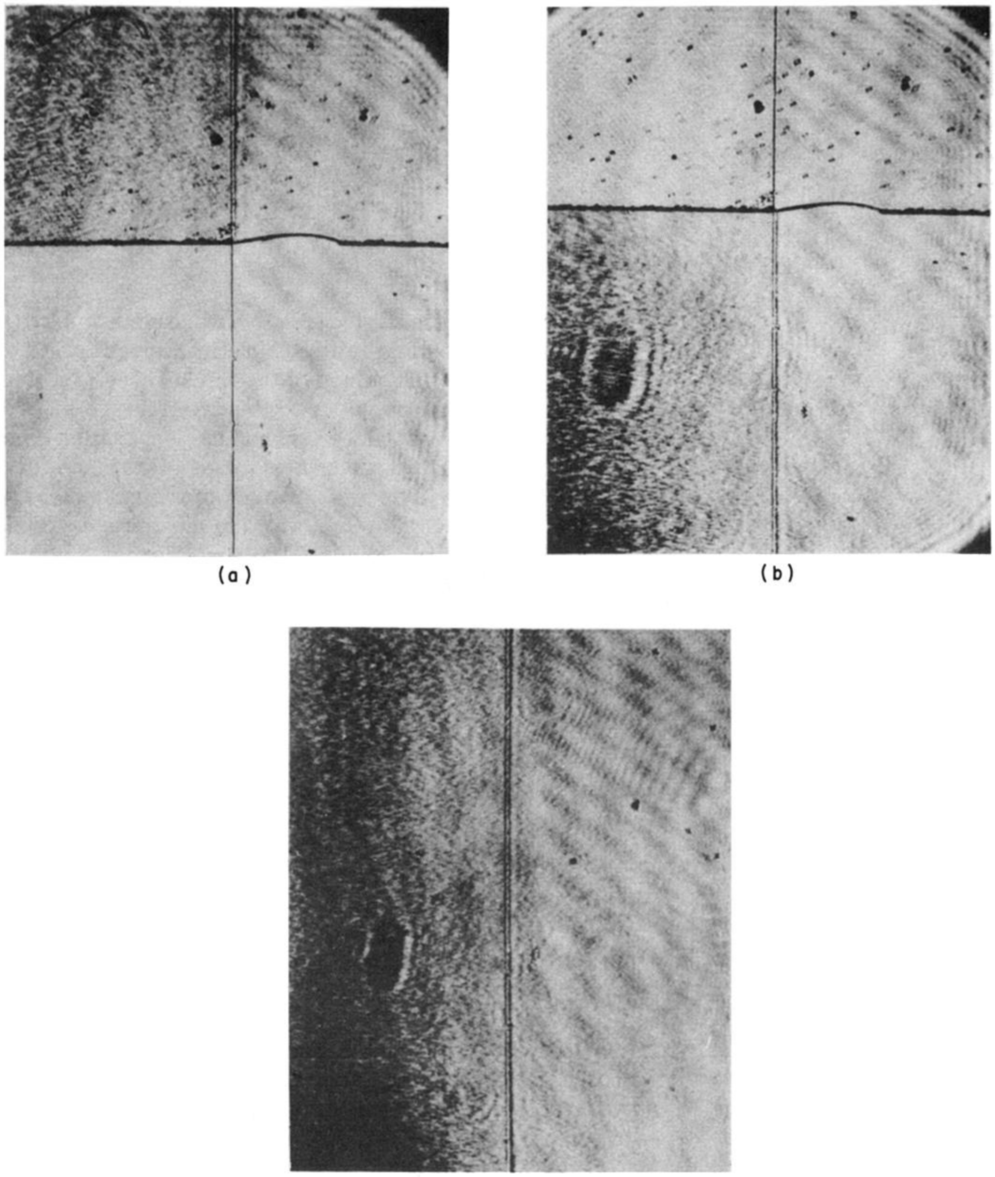

FIG. 14. Photographic recording of the longitudinal shift, where (a) above shows the TE mode and below the TM mode, (b) above shows the TM mode and below the TE mode, and (c) shows the linear polarization at 45°.

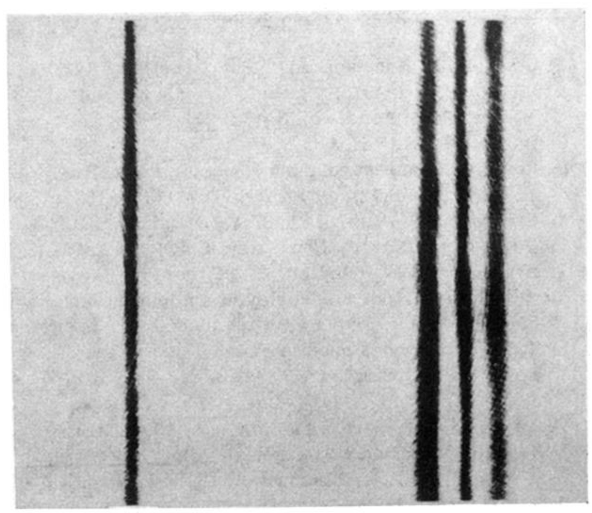

(a) (b)

FIG. 19. Photographic recording of the transverse shift with a Wolter plate as object for (a) nonresonant and (b) resonant reflection, showing a nonshifted and two shifted images. The measured value of the transverse shift, that is, the distance between the two lateral lines and the central one, is 30 $\mu \pm 2\%$.

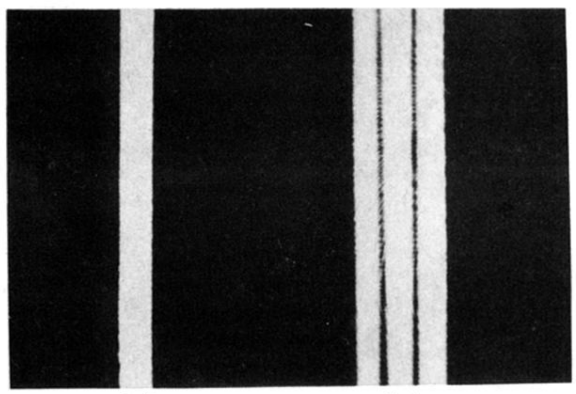

FIG. 20. Photographic recording of the transverse shift (same as Fig. 19), but with a narrow slit replacing the Wolter plate. This photograph has not been used for measuring the transverse shift.